Inorganic Chemistry

Article

pubs.acs.org/IC

Tris(5-methylpyrazolyl)methane: Synthesis and Properties of Its Iron(II) Complex

Margaret A. Goodman,[†] Alexander Y. Nazarenko,[‡] Barbara J. Casavant,[‡] Zhanjie Li,[‡] William W. Brennessel,[§] Michael J. DeMarco,[⊥,∥] Gen Long,[∥] and M. Scott Goodman*[,‡]

[†]Department of Math and Natural Sciences, D'Youville College, Buffalo, New York 14201, United States

[‡]Department of Chemistry and [⊥]Department of Physics, Buffalo State College, Buffalo, New York 14222, United States

[§]Department of Chemistry, University of Rochester, Rochester, New York 14627, United States

[∥]Department of Physics, SUNY at Buffalo, Buffalo, New York 14260, United States

Supporting Information

ABSTRACT: The new ligand, tris(5-methylpyrazolyl)-methane (**1**), has been prepared by the reaction of *n*-butyl lithium with tris(pyrazolyl)methane followed by trimethylation of the tetralithiated species with methyl iodide. The BF_4^-, ClO_4^-, and BPh_3CN^- salts of the Fe(II) complex of this ligand were also synthesized. The X-ray crystal structure of the BF_4^- complex (**2**) at 100 K had Fe−N bond lengths of 1.976 Å, indicative of a low spin Fe(II) complex, while at room temperature, the structure of this complex had a Fe−N bond distance close to 2.07 Å, indicative of an admixture of approximately 50% low-spin and 50% high-spin. The solid-state structure of the complex with a ClO_4^- counterion was determined at 5 different temperatures between 173 and 293 K, which allowed the thermodynamic parameters for the spin-crossover to be estimated. Mössbauer spectra of the BF_4^- complex further support spin-state crossover in the solid state with a transition temperature near 300 K. UV−visible spectroscopy and ^1H NMR studies of **2** show that the transition temperature in solution is closer to 400 K. No spin-crossover was observed for $[Fe(\mathbf{1})_2]^{2+}\cdot 2BPh_3CN^-$. The results allow the separation of effects of groups in the 3-position from those in the 5-position on tpm ligands, and also point toward a small cooperative effect in the spin-crossover for the Fe(II) complex.

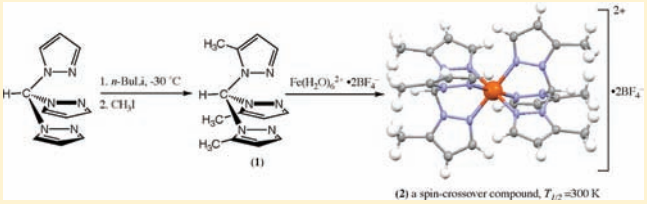

INTRODUCTION

The tris(pyrazolyl)borates (tp) and tris(pyrazolyl)methanes (tpm) are well-known examples of tripodal, nitrogen-donor ligands.[1] These ligands, sometimes referred to as "scorpionates", consist of a boron (tp) or a carbon (tpm) atom bonded simultaneously to three pyrazole moieties through a bond to a pyrazole ring nitrogen, with the fourth group on the central boron or carbon atom typically being a hydrogen. The second nitrogen on each of the three pyrazoles is then available for chelating to a metal ion (Figure 1). The tp and tpm ligands behave quite similarly with respect to metal binding, with most differences easily accounted for by the fact that tp is anionic whereas tpm is generally neutral. Even this difference has been somewhat mitigated by the introduction of monoanionic tpm ligands, especially the elegant work of Breher and coworkers.[2]

While complexes of these ligands with metals from across the periodic table are known, Fe(II) complexes of tp and tpm ligands have been particularly well-studied.[3] With Fe(II), these tp and tpm ligands generally form pseudo-octahedral complexes containing two tridentate ligands, provided that the substituents in the 3-position of the pyrazoles (Figure 1, R_1) are not so sterically demanding as to preclude the necessary interdigitation of these groups in the octahedral complex. The Fe(II) complexes may also exhibit temperature-dependent spin-states

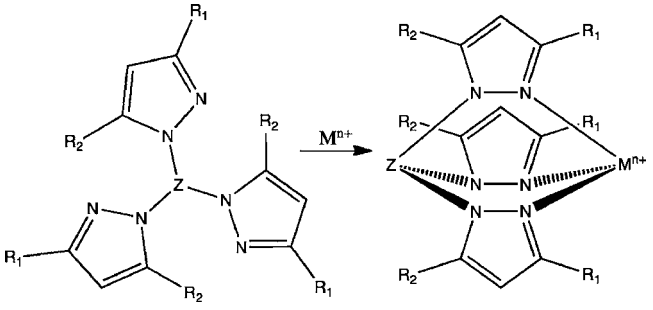

Figure 1. Tris(pyrazolyl)borates: Z = BH^-; tris(pyrazolyl)methanes: Z = CH.

in both the solid state and in solution.[4] Since Fe(II) has a $3d^6$ electronic configuration, octahedral complexes of Fe(II) can have either a high-spin (HS, $S = 2$) or a low-spin (LS, $S = 0$) ground-state electronic configuration. The transition between the paramagnetic HS state and the diamagnetic LS state can occur gradually or abruptly, with the transition temperature being somewhat correlated with the nature of the substituents

Received: October 11, 2011
Published: December 23, 2011

   dx.doi.org/10.1021/ic2022038 | *Inorg. Chem.* 2012, 51, 1084−1093

Chart 1. Structure of Tris(5-methylpyrazolyl)methane (1) and Its Fe(II) Complex 2

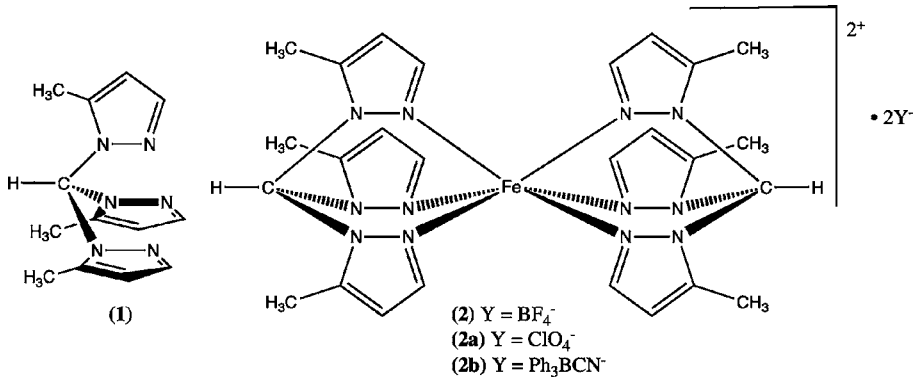

on the pyrazoles. This has several potential applications including, but not limited to, switches, wires, and temperature threshold indicators.[5]

Tpm ligands with a variety of different substituents on the pyrazole rings have been synthesized. Largely because of synthetic constraints, the most commonly encountered substitution pattern places groups exclusively in the 3-positions of the pyrazole (Figure 1, R_1 = alkyl, aryl, etc.; R_2 = H).[6a] Because the substituents in the 3-position approach each other closely upon 2:1 complex formation, these substitutents can impart dramatic effects on the structure and properties of the corresponding metal complexes. For example, when the substituent in the 3-position is sufficiently bulky (as in the so-called "2nd generation" tpms), the ligand will only reluctantly form 2:1 ligand/metal complexes, or as is often the case, form complexes with 1:1 ligand/metal stoichiometry or complexes containing incomplete coordination of the pyrazole nitrogens.[6b]

Another frequently encountered substitution pattern is with groups in both the 3- and 5-positions of the pyrazoles. These groups are either identical (e.g., Figure 1, $R_1 = R_2 = CH_3$ or *i*Pr) or the substituent in the 3-position is larger than the one in the 5-position (e.g., Figure 1, R_1 = Ph; $R_2 = CH_3$).[6] This again is the result of synthetic constraints. Additionally, ligands with a group solely in the 4-position and with groups in the 3-, 4-, and 5-positions have been described.[6c]

As a result of our interest in the chemistry of compounds that exhibit spin-state transitions near room temperature, we undertook the synthesis of a tpm ligand with a substitution pattern that has, thus far, not been described for tris-pyrazole ligands. Herein we report the synthesis of compound **1** (Chart 1), a very simple tpm ligand with substitution exclusively in the 5-position, and its Fe(II) complex (**2**, Chart 1). The properties of its cationic complex with Fe(II) is also described using a combination of X-ray crystallography, spectroscopic measurements, and Mössbauer. These studies have allowed us to isolate the effect of a substituent in the 5-position and once again confirm that small changes in the steric demands of a tpm ligand and the identity of the (counter) anion can cause significant changes in the structural properties, especially the spin-state transition characteristics, of Fe(II) complexes of tris-pyrazole ligands.

EXPERIMENTAL SECTION

General Procedures. All solvents were reagent grade and were used without further purification, except tetrahydrofuran (THF), which was distilled from Na–K alloy under argon. Methyl iodide, butyllithium (2.5 M in hexanes), and iron(II) tetrafluoroborate hexahydrate were purchased from Acros Organics, and sodium triphenylcyanoborate was obtained from Apolda (Germany), and were used without further purification. Tris(pyrazolyl)methane[6a] was prepared according to the literature.

NMR spectra were recorded on a Bruker Avance 300 at a field of 300 MHz for protons, and all chemical shifts are reported relative to TMS. FTIR spectra were recorded on a Thermo-Nicolet Nexus 470 and GC-MS data were recorded on a Thermo-Finnigan Trace DSQ instrument. Dispersive Raman spectra were collected on a Bruker Senterra Raman microscope (see Supporting Information) and UV–visible spectra were acquired on an HP 8453 single beam spectrophotometer using acetonitrile as a blank.

Synthesis of Tris(5-methylpyrazolyl)methane (1). Tris(pyrazolyl)methane (0.96 g, 4.5 mmol) in dry THF (9 mL) was cooled to −30 °C (acetonitrile/dry ice) under Argon. Butyllithium (2.5 *M* in hexanes, 9 mL, 22.5 mmol, 5.0 equiv) was carefully added, and the reaction allowed to stir for 1 h. The mixture was then cooled to −78 °C (acetone/dry ice), and methyl iodide (1.4 mL, 22.5 mmol, 5.0 equiv) was added slowly with efficient stirring over 5 min. The reaction mixture was stirred for an additional 1 h at −78 °C and then allowed to warm to 0 °C over a period of 2 h. The reaction was carefully quenched with a few drops of methanol and allowed to warm to room temperature. Volatiles were removed by rotary evaporation, and the resulting material was dissolved in CH_2Cl_2 (25 mL) and washed twice with water (10 mL) to remove excess lithium salts. The CH_2Cl_2 layer was dried with Na_2SO_4 and evaporated. Pure compound **1** was obtained by crystallization of the residue from toluene/hexanes (1:1). Yield: 0.75 g (65% yield); mp: 145–148 °C; Anal. Calcd. for $C_{13}H_{16}N_6$: C, 60.92; H, 6.29; N, 32.79. Found: C, 60.89; H, 6.34; N, 33.02; ^{1}H NMR ($CDCl_3$) δ 8.31 (s, 1H), 7.51 (d, J = 1.5 Hz, 3H), 6.14 (d, J = 0.81, 0.81 Hz, 3H), 2.09 (s, 9H); ^{13}C NMR ($CDCl_3$) δ 140.2, 107.8, 80.9, 30.9, 10.7; IR (diamond ATR, cm^{-1}) 3132, 2952, 2933, 1551, 1420, 1352, 1288, 1216, 1097, 883. The sample was pure as judged by a single peak in the EI GC/MS m/z (rel. % abund.) = 256 (M^+, 1), 173 (100) (GC conditions: inj. 150 °C, column program: initial temp. 150 °C, 2 min hold, ramp 15 °C/min., final temp. 225 °C, ion source: 250 °C, 70 eV).

Preparation of the Fe(II) Complex, $[Fe(1)_2]^{2+}\cdot 2BF_4^-$ (2). Tris(5-methylpyrazolyl)methane (**1**) (0.275 g, 1.07 mmol) was dissolved in dry THF (4 mL) under argon. In a separate flask, iron(II) tetrafluoroborate hexahydrate (0.173 g, 0.51 mmol) was dissolved in dry THF (1 mL) under argon. The tpm/THF solution was then added to the Fe(II)/THF solution via syringe, and the mixture was stirred for 1 h at room temperature. The product, a fine, purple powder was isolated by filtration, rinsed with fresh THF, and allowed to air-dry. The complex could be crystallized by dissolution in CH_3CN and allowing CH_2Cl_2 or $CHCl_3$ to slowly diffuse into the solution. This produced high quality crystals that desolvated within seconds upon removal from the mother liquor. Alternatively, slow evaporation of a CH_3CN solution of the complex also produced X-ray quality crystals, but without incorporation of loosely bound solvent. ^{1}H NMR (CD_3CN) δ 7.79 (s, 1H), 7.49 (s, 3H), 6.84 (s, 3H), 2.99 (s, 9H); ^{13}C NMR ($CDCl_3$, 21 °C) δ 159.6, 154.2, 115.1, 67.3, 11.4; IR

dx.doi.org/10.1021/ic2022038 | *Inorg. Chem.* 2012, 51, 1084–1093

(diamond ATR, cm^{-1}) 3158, 1477, 1449, 1298, 1246, 1054, 1022, 983, 944, 810, 649, 519.

X-ray Crystallography, General Information. Initial evaluation of the crystal, unit cell determination, and X-ray intensity data measurement were performed using a Bruker SMART APEX II CCD Platform diffractometer. Crystals were mounted onto the tip of a 0.1 mm diameter glass fiber for data collection at the desired temperature. The data collection was carried out using MoKα radiation (graphite monochromator). A randomly oriented region of reciprocal space was surveyed: three major sections of frames were collected with 0.50° steps in ω at three different ϕ settings and a detector position of −33° in 2θ. The intensity data were corrected for absorption.[7] The space groups were determined based on systematic absences and intensity statistics, and the structures were solved using SIR97[8] and refined using SHELXL-97.[9] A direct-methods solution was calculated, which provided most non-hydrogen atoms from the E-map. Full-matrix least-squares/difference Fourier cycles were then performed, which located the remaining non-hydrogen atoms. All non-hydrogen atoms were refined with anisotropic displacement parameters. All hydrogen atoms were placed in ideal positions and refined as riding atoms with relative isotropic displacement parameters.

Structure of 2. The crystal (0.16 × 0.14 × 0.02 mm^3) was analyzed at 100.0(1) K and 293(2) K. The X-ray crystallographic data for **2** are given in Table 1.

Table 1. Crystallographic Data for the Structural Analyses of 2

parameter	100 K	293 K
empirical formula	$C_{26}H_{32}B_2F_8FeN_{12}$	$C_{26}H_{32}B_2F_8FeN_{12}$
formula weight, g/mol	742.11	742.11
space group	$R\bar{3}$	$R\bar{3}$
$a = b$, Å	10.9589(14)	11.1820(9)
c, Å	21.280(5)	21.578(3)
$\alpha = \beta$, deg	90	90
γ, deg	120	120
volume, $Å^3$	2213.3(9)	2336.6(6)
Z	3	3
ρ(calcd), Mg/m^3	1.670	1.582
absorption coefficient, mm^{-1}	0.606	0.574
crystal color	purple	pale pink
final R, wR^2 [$I > 2\sigma(I)$]	0.0328, 0.0754	0.0395, 0.0983

Structure of $[Fe(1)_2]^{2+}\cdot 2ClO_4^-$ (2a). To prepare the crystals, complex **2** (30 mg) along with $NaClO_4$ (15 mg, 3 equiv) were dissolved in CH_3CN (200 μL). The sample was kept in a sealed container at room temperature for 1 week. Elongated, colorless plates of $NaBF_4$ were deposited during this time, along with purple crystals of the perchlorate complex.

The crystal (0.22 × 0.14 × 0.08 mm^3) was analyzed at 173.0(2) K, 243.0(2) K, 263.0(2) K, 283.0(2) K, and 300.0(2) K. A summary of the X-ray crystallographic data is given in Table 2.

Structure of $[Fe(1)_2]^{2+}\cdot 2Ph_3BCN^-$ (2b). To prepare the crystals, complex **2** (30 mg) along with sodium triphenylcyanoborate (32 mg, 3 equiv) were dissolved together in CH_3CN (200 μL). The sample was left in a sealed container overnight, during which time large purple crystals suitable for X-ray diffraction were deposited.

The crystal (0.24 × 0.20 × 0.10 mm^3) was analyzed at 100.0(1) K. A summary of the X-ray crystallographic data is given in Table 3.

Table 3. Crystallographic Data for the Structural Analyses of $[Fe(1)_2]^{2+}\cdot 2Ph_3BCN^-$ (2b)

parameter	value
empirical formula	$C_{68}H_{68}B_2FeN_{16}$
formula weight, g/mol	1186.85
space group	$P2_1/c$
a, Å	14.6268(17)
b, Å	10.0287(12)
c, Å	22.086(2)
$\alpha = \gamma$, deg	90
β, deg	109.064(7)
volume, $Å^3$	3062.1(6)
Z	2
ρ(calcd), Mg/m^3	1.287
absorption coefficient, mm^{-1}	0.303
crystal color	purple
final R, wR^2 [$I > 2\sigma(I)$]	0.0343, 0.0927

Mössbauer Spectroscopy. The Mössbauer experiments on **2** were performed in vertical transmission geometry inside the sample chamber of a cryostat with both the source, ^{57}Co(Rh), and sample held at the same temperature in a gas bath.[10] The velocity calibration was performed with α-Fe foil and isomer shifts are referenced to the foil. The delrin sample holder contained a total of 0.2 mg/cm^2 of ^{57}Fe for the sample. The Mössbauer γ-ray was detected by a proportional counter placed below the cryostat mylar window. The sample was measured first at room temperature, 298 K, and then cooled to 77 K for low temperature data collection.

RESULTS

Synthesis of Compound 1. Tpm ligands are generally synthesized by the action of pyrazole on chloroform.[6] Substituted pyrazoles lead to a mixture of tpm regioisomers if the groups on the 3- and 5-position of the pyrazole are different. The ratio of the 4 possible (kinetic) products in the

Table 2. Crystallographic Data for the Structural Analyses of $[Fe(1)_2]^{2+}\cdot 2ClO_4^-$ (2a)

parameter	173 K	243 K	263 K	283 K	300 K
empirical formula	$C_{26}H_{32}Cl_2FeN_{12}O_8$	$C_{26}H_{32}Cl_2FeN_{12}O_8$	$C_{26}H_{32}Cl_2FeN_{12}O_8$	$C_{26}H_{32}Cl_2FeN_{12}O_8$	$C_{26}H_{32}Cl_2FeN_{12}O_8$
formula weight, g/mol	767.39	767.39	767.39	767.39	767.39
space group	$R\bar{3}$	$R\bar{3}$	$R\bar{3}$	$R\bar{3}$	$R\bar{3}$
$a = b$, Å	11.0644(12)	11.1522(12)	11.1783(10)	11.1948(7)	11.2103(6)
c, Å	21.420(5)	21.492(5)	21.515(4)	21.613(3)	21.708(2)
$\alpha = \beta$, deg	90	90	90	90	90
γ, deg	120	120	120	120	120
volume, $Å^3$	2270.9(8)	2314.9(8)	2328.2(7)	2345.7(5)	2362.6(4)
Z	3	3	3	3	3
ρ(calcd), Mg/m^3	1.683	1.651	1.642	1.630	1.618
absorption coeff., mm^{-1}	0.748	0.734	0.729	0.724	0.719
crystal color	purple	purple	purple	pink	pale pink
final R, $wR2$ [$I > 2\sigma(I)$]	0.0385, 0.1195	0.0464, 0.1448	0.0479, 0.1540	0.0496, 0.1668	0.0510, 0.1779

dx.doi.org/10.1021/ic2022038 | Inorg. Chem. 2012, 51, 1084−1093

crude reaction mixture not only depends on the relative steric bulk of the two substituents, but also on statistical considerations, with the less symmetrical products being favored in this case. The larger of the two substitutents always prefers the less-hindered 3-position of the product, and it is possible to exploit this tendency to simplify the product mixture. Acid-catalyzed equilibration of the initially formed product mixture results in nearly exclusive formation of the isomer with the larger substituents in the 3-position.

When 3(5)-methylpyrazole is utilized in the standard tpm-forming reaction, all four possible regioisomers are formed, as expected, with the 3,3,5-trimethyl isomer being the major product (Figure 2). The crude reaction mixture also contains

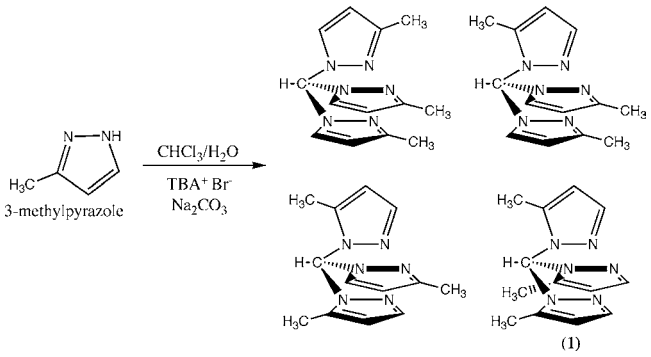

Figure 2. Classic synthesis of a tpm ligand using 3-methylpyrazole results in the formation of all four possible regioisomers.

substantial amounts of the 3,3,3-trimethyl isomer along with lesser amounts of the 3,5,5-trimethyl and 5,5,5-trimethyl isomer (**1**) as judged by ^{1}H NMR (see Supporting Information). This reaction mixture can be isomerized, resulting in a two-component mixture containing the 3,3,5-trimethyl isomer as the major product and a slightly lesser amount of the 3,3,3-trimethyl isomer. The methyl substituents, while still preferring the 3-position over the 5-position, are simply not sterically demanding enough to overcome the statistical preference for the 3,3,5 isomer.

The presence of a significant amount of a 5,5,5-substituted isomer, such as **1**, in a tpm reaction mixture is actually an uncommon occurrence, so in this case it should be possible to isolate and purify ligand **1** by this method. While in our hands it was indeed possible to isolate **1** from this mixture, the procedure involved exhaustive recrystallizations and repeated chromatography steps that lead only to trace amounts of **1** in an irreproducible manner.

Instead, a much more reliable and effective approach to the synthesis of **1** was developed. This method involves selective trimethylation of a tetralithiated tris(pyrazolyl)methane as depicted in Figure 3. Because of the adjacency of 3 nitrogen heterocycles, the apical hydrogen of the tpm is somewhat acidified, such that it is possible to selectively deprotonate this position at −78 °C using 1 equivalent of an alkyllithium. This fact has been used numerous times to produce a variety of tpm ligands substituted at the methine carbon.[11] Moreover, it has been recently reported that the monoanion produced by treatment of tris(3,5-dimethylpyrazolyl)methane with methyllithium is actually quite stable, and a variety of metal complexes of the anionic dimethyl tpm have now been synthesized and characterized.[2]

If on the other hand, an excess of *n*-butyllithium is used and the lithiation reaction run at slightly higher temperature (−30 °C), clean tetralithiation to produce intermediate **3** can be achieved. The exact nature of this tetralithiated material is unknown, but it is unlikely to be as simple as the structure shown in Figure 3 since the tridentate tpm ligand and THF solvent are both perfectly capable of coordinating to lithium ions. The existence of the tetralithiated intermediate **3** was confirmed by quenching experiments with D_2O followed by NMR analysis of the deuterated product (see Supporting Information).

Treatment of **3** with excess methyl iodide at −78 °C leads to the selective methylation of only the 5-positions of each pyrazole, with negligible methylation of the apical carbon. Apparently substitution at even one of the 5-positions renders the apical carbon too sterically hindered to be methylated at an appreciable rate. After that occurrence, each successive addition of a methyl group to a 5-position of another pyrazole ring further hinders substitution at the apical carbon, such that it becomes impossible to methylate the methine carbon at all once all three of the 5-positions are occupied by a methyl group. Even after extended methylation times (3 days), only very small amounts of the tetramethylated compound could ever be observed by GC-MS. This lack of reactivity was observed previously by Reger during his unsuccessful attempt to methylate tris(3,5-dimethylpyrazolyl)methane.[12] In our studies, if an insufficient amount of *n*-butyllithium was used, products derived from partial methylation at both the methine carbon and the 5-positions of the pyrazoles were sometimes produced. A similar pattern of reactivity was noted previously with bis(pyrazolyl)methanes,[13] where it was observed that methylation of the central carbon could occur even after both 5-positions of the adjacent pyrazoles had been methylated.

Temperature seems to be an important variable for success of this reaction. From the previously mentioned quenching studies, complete tetralithiation required at least 30 min at −30 °C; at −78 °C the monolithiated product was the major lithiated species, and full conversion to **3** was not achieved even after extended reaction times with excess *n*-butyllithium. After lithiation, the reaction mixture was cooled to −78 °C before

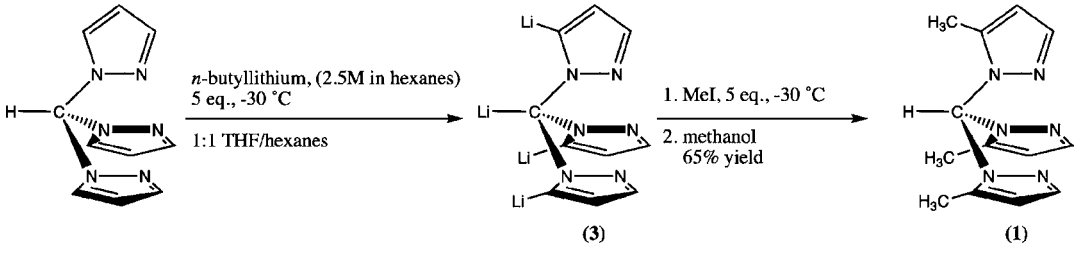

Figure 3. Alternative synthesis of tris(5-methylpyrazolyl)methane (**1**).

dx.doi.org/10.1021/ic2022038 | Inorg. Chem. 2012, 51, 1084−1093

addition of methyl iodide to help control the reactivity and selectivity of the methylation step. Control of the initial methylation is crucial for success of the reaction; as stated previously, once reaction has occurred at the 5-position of one of the pyrazole rings, subsequent methylation reactions occur almost exclusively on the remaining pyrazole rings.

Finally, the sheer amount of lithium ion present leads to some difficulties removing all of it from the product during workup. Several washes with deionized water were found to be necessary to afford the pure ligand completely free from lithium ion.

Solid State Studies of 2. When 2 equiv of ligand **1** are mixed with an equivalent of $Fe(BF_4)_2{\cdot}6H_2O$ in THF, the Fe(II) complex, $[Fe(\mathbf{1})_2]{\cdot}2BF_4$ (**2**) precipitates almost instantly. The complex initially formed is a light violet color. It is well-known that LS Fe(II) complexes of tpm ligands are violet and HS complexes are colorless.[5b,14a] Thus, the initial visual evidence suggests that **2**, with its BF_4^- counterion, has a LS electron configuration.

Crystals of **2** can be easily grown by first dissolving the crude material in acetonitrile to give a purple solution, and subsequently exposing this solution to vapors of methylene chloride or chloroform. Under these conditions the most abundant crystals, although apparently perfectly formed, were highly solvated by weakly bound chloroform or methylene chloride and proved to be exceedingly difficult to collect high quality X-ray data on (the crystals degraded almost instantly upon removal from the solution). However, preliminary X-ray data on these violet crystals did indicate Fe−N bond lengths of 1.98 Å, characteristic of a LS complex at 100 K. There were 2 molecules of solvent present for every $[Fe(\mathbf{1})_2]^{2+}$ unit.

Careful examination of the crystallization vial also revealed violet crystals with somewhat different morphology. These crystals of **2** could be grown more consistently by simply allowing an acetonitrile solution of the complex to slowly evaporate. These were stable in air and were quite amenable to X-ray analysis. The structure determined at 100 K is shown in Figure 4. The structure reveals Fe−N bond distances of 1.976

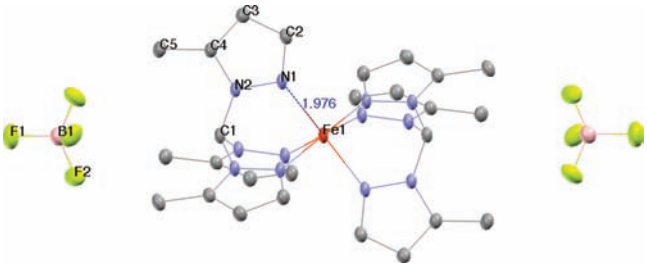

Figure 4. Crystal structure of **2** at 100 K. The Fe−N bond lengths are 1.976 Å, indicative of a LS Fe(II) complex. Solvent molecules and are not shown.

Å, all of which are equivalent because of symmetry constraints of the spacegroup ($R\bar{3}$). The intraligand N−Fe−N bond angles are each 87.11°, while the interligand N−Fe−-N bond angles are each 92.89° (Table 1). These angles indicate that the N_6-coordination geometry is only slightly distorted from octahedral. The unit cell contains 3 complexes, two acetonitriles per complex, and slightly disordered BF_4^- ions situated around the 3-fold symmetry axis.

There are several parameters that can be used to describe octahedral distortion (Supporting Information, Table S2).[15] In particular, Reger has correlated the pyrazole twist angle (τ), measured as the Fe−N1−N2−C1 dihedral, in tpm (and tp) complexes of Fe(II) with the LS/HS transition temperature.[4a,b,16] In the present case, the value of τ is 10.54°. This angle is unusually large for a LS complex of this type, which often have τ values between 1° and 2°. The three methyl groups of each ligand are oriented parallel to each other and are forced into somewhat close proximity with each other and the methine C−H by the complexation process. Twisting of the pyrazole rings results in the methyl groups moving farther apart and slightly away from the methine hydrogen, and this could account for the unusually high "twist" angle of the pyrazoles in this LS complex.

To investigate whether this complex would display spin-state crossover behavior in the solid state, a structure for the same crystal was also determined at 293 K. In this case, Fe−N bond lengths increased to 2.071 Å, indicating a LS/HS mixture of approximately 50% each in the crystal near room temperature. There is also a distinct elongation of the complex along the C1−Fe−C1 axis, resulting in a distortion away from octahedral coordination geometry. The intraligand N−Fe−N bond angles are now each 85.08°, while the interligand N−Fe−N bond angles are each 94.92° (Table 4). The pyrazole twist angle τ has

Table 4. Selected Bond Distances and Bond Angles for 2

	temperature	
	100 K	293 K
	Bond Distances (Å)	
Fe−N(1)	1.976(2)	2.071(2)
N(1)−C(2)	1.323(3)	1.317(3)
N(1)−N(2)	1.371(2)	1.370(2)
N(2)−C(4)	1.366(2)	1.363(3)
N(2)−C(1)	1.442(2)	1.444(2)
C(2)−C(3)	1.399(2)	1.384(3)
C(3)−C(4)	1.366(2)	1.359(3)
C(4)−C(5)	1.500(2)	1.493(3)
	Bond Angles (deg)	
N(1)−Fe−N(1)#1	180.00(6)	180.00(7)
N(1)−Fe−N(1)#2	92.89(7)	94.92(8)
N(1)−Fe−N(1)#3	87.11(7)	85.08(8)
N(2)−C(1)−N(2)′	109.8(2)	110.4(2)

also increased to 11.21°. Since there is a substantial contribution from both LS and HS forms contributing to the measured angles in this structure, the "pure" HS complex must be significantly distorted from octahedral and have τ >12°. Although the difference between the HS and LS torsion angle is smaller than previously seen for complexes like this, the direction of change again confirms Reger's previous results.

Solid State Studies of 2a. A very similar set of crystal structures was obtained when the BF_4^- anion was replaced with the ClO_4^- ion. Mixing a slight excess of $NaClO_4$ with an acetonitrile solution of **2** resulted in slow deposition of X-ray quality crystals of the perchlorate salt of the Fe(II) complex (**2a**). The X-ray structure of **2a** at 173 K was nearly indistinguishable from the $[Fe(\mathbf{1})_2]^{2+}$ ion in **2** at 100 K. For example, they both possess the same trigonal crystal system with identical space groups, $R\bar{3}$. Additionally, all Fe−N bond distances are 1.976 Å (Table 5).

In the case of **2a**, high-quality crystal structures were also determined at several other temperatures (243 K, 263 K, 283 K, and 300 K; Table 5). The results show that as the temperature

dx.doi.org/10.1021/ic2022038 | Inorg. Chem. 2012, 51, 1084−1093

Table 5. Selected Bond Distances and Bond Angles for 2a

	temperature				
	173 K	243 K	263 K	283 K	300 K
		Bond Distances (Å)			
Fe−N(1)	1.976(2)	1.984(2)	1.997(2)	2.034(2)	2.073(2)
N(1)−C(2)	1.328(3)	1.325(3)	1.327(3)	1.322(3)	1.319(4)
N(1)−N(2)	1.373(2)	1.374(2)	1.372(2)	1.374(2)	1.372(2)
N(2)−C(4)	1.364(2)	1.361(3)	1.359(2)	1.356(3)	1.357(3)
N(2)−C(1)	1.443(2)	1.444(2)	1.444(2)	1.445(2)	1.445(2)
C(2)−C(3)	1.404(2)	1.402(3)	1.397(3)	1.396(4)	1.395(4)
C(3)−C(4)	1.374(2)	1.364(3)	1.363(3)	1.365(3)	1.369(4)
C(4)−C(5)	1.494(2)	1.498(3)	1.493(3)	1.489(3)	1.490(3)
		Bond Angles (deg)			
N(1)−Fe−N(1)#1	180.00(7)	180.00(8)	180.00(8)	180.00(8)	180.00(9)
N(1)−Fe−N(1)#2	87.00(6)	86.80(8)	86.49(8)	85.85(8)	85.12(8)
N(1)−Fe−N(1)#3	93.00(6)	93.20(8)	93.51(8)	94.15(8)	94.88(8)
N(2)−C(1)−N(2)#3	109.9(2)	110.0(2)	110.2(2)	110.5(2)	110.9(2)

is increased, the Fe−N bond distances increase slowly and smoothly, as expected for a spin-state crossover compound that is undergoing spin-state crossover without significant cooperativity. At 300 K, the highest temperature obtainable, the Fe−N bond distance is very close to 2.07 Å, which is approximately halfway between the LS value of 1.97 Å and the expected value for a HS complex (ca. 2.17 Å).[14] Thus, the transition temperature is very near room temperature for this complex/anion combination.

Further analysis is possible by plotting the Fe−N bond distance in **2a** versus temperature; the result is shown in Figure

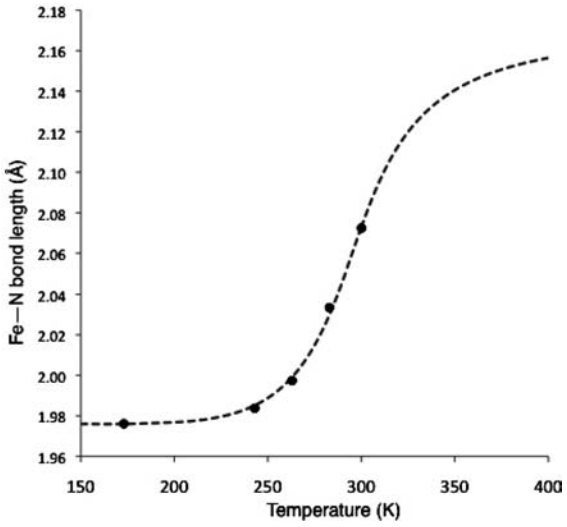

Figure 5. Plot of the Fe−N bond length as a function of temperature from the variable temperature X-ray analysis of **2a**. The dotted line was produced from eq 1 using the parameters ΔH° = +20.0 kJ/mol, ΔS° = +66.7 J/mol-K, $Fe{-}N_{LS}$ = 1.976 Å, $Fe{-}N_{HS}$ = 2.169 Å, and Γ = +2.50 kJ/mol is included.

5. When a simple thermodynamic equation (van't Hoff type) describing the simple HS/LS spin equilibrium was fit to the data points, assuming a LS bond length $(Fe{-}N)_{LS}$ of 1.96 Å, the result is a very good fit with the following parameters: HS bond length $(Fe{-}N)_{HS}$ 2.17 Å, ΔH° = +36.6 kJ/mol, and ΔS° = +122 J/mol-K. The calculation also gives a transition temperature ($T_{1/2} = \Delta H^\circ/\Delta S^\circ$) near 300 K for this complex in the solid state. The LS to HS transition is driven by entropy, as might be expected for a spin change from $S = 0$ to $S = 2$ (ca. 13 J/mol-K) and significant lengthening and weakening of the Fe−N bonds. Accordingly, at temperatures near room temperature, this complex exists as a nearly 50:50 mixture of the HS and LS forms in rapid equilibrium. While the calculated value for $Fe{-}N_{HS}$ is satisfyingly close to that observed in the crystal structures of other, similar HS complexes,[14,16] this method gave estimates for the basic thermodynamic values, ΔH° and ΔS°, that are well outside the expected range for a spin transition of this type.[17] For example, the thermodynamic values calculated in a previous report for the related $\{Fe[HC(pz)_3]_2\}(BF_4)_2$ complex were ΔH° = +20 kJ/mol, and ΔS° = +58 J/mol-K.[4f] Thus, it appears that there is some cooperativity in the spin crossover behavior of the present complexes that is not accounted for in the simple model. Instead, the model of Slichter and Drickamer[18] was considered, which uses eq 1 to take into account the cooperativity.

$$\ln\left(\frac{1-c}{c}\right) = \frac{\Delta H + \Gamma(1-2c)}{RT} - \frac{\Delta S}{R} \qquad (1)$$

In this equation, Γ is a measure of the cooperativity of the LS→HS transition and c is the molar fraction of HS component calculated using eq 2 and the X-ray crystallographic bond lengths (Fe−N).

$$c = [(Fe{-}N)_{obs} - (Fe{-}N)_{LS}]/[(Fe{-}N)_{HS} - (Fe{-}N)_{LS}] \qquad (2)$$

While a careful fit of eq 1 to the data was not performed, primarily because only 5 data points covering only half of the spin-state transition were measured, Figure 5 shows a plot of eq 1 that utilizes reasonable thermodynamic values and Fe−N bond lengths (ΔH° = +20.0 kJ/mol, ΔS° = +66.7 J/mol-K, $(Fe{-}N)_{LS}$ = 1.976 Å, $(Fe{-}N)_{HS}$ = 2.169 Å). These parameters were carefully chosen to give a $T_{1/2}$ of 300 K, a value supported by the previous van't Hoff analysis and bond length measurements in numerous Fe-tpm complexes of this type.[4f,17] This analysis also assumes no changes in either ΔH° or ΔS° over the large temperature range of the spin transition. Using these values, the best fit to the data results when Γ = 2.5 kJ/mol, which confirms that cooperativity is indeed a factor in this spin-state transition. The observations on

dx.doi.org/10.1021/ic2022038 | Inorg. Chem. 2012, 51, 1084−1093

the BF_4^- salt suggests a very similar transition temperature for **2**, and probably very similar thermodynamic parameters.

Solid State Studies of 2b. Crystals of $[Fe(\mathbf{1})_2]^{2+}$ cation with the bulky anion, triphenylcyanoborate (BPh_3CN^-), can be readily grown by codissolving the tetrafluoroborate salt **2** with $NaBPh_3CN$ in acetonitrile. Large purple crystals of $[Fe(\mathbf{1})_2]^{2+}\cdot 2BPh_3CN^-$ (**2b**), suitable for X-ray structure determination, are quickly deposited upon standing. The X-ray structure determined at 100 K is shown in Figure 6. The

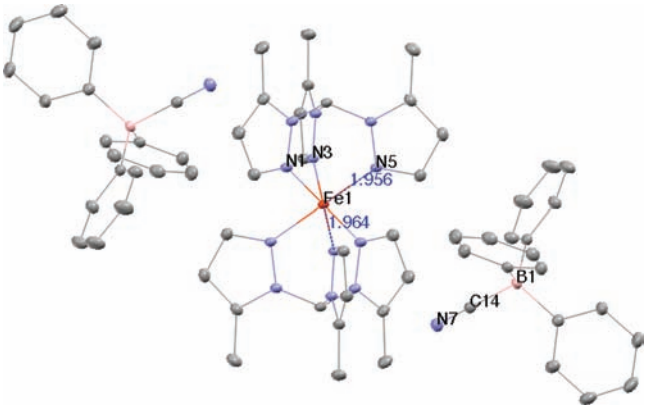

Figure 6. Structure of **2b** at 100 K. Two acetonitrile molecules in the structure are not shown.

cationic complex in this crystal possesses symmetry (space group = $P2_1/c$) that results in three different Fe–N bond lengths, which are all close to 1.96 Å (Table 6). This is exactly

Table 6. Selected Bond Distances and Bond Angles for 2b

	temperature
	100 K
Bond Distances (Å)	
Fe–N(1)	1.964(1)
Fe–N(3)	1.964(1)
Fe–N(5)	1.956(1)
N(2)–C(1)	1.440(2)
N(4)–C(1)	1.440(2)
N(6)–C(1)	1.448(2)
Bond Angles (deg)	
N(1)–Fe–N(1)#1	180.00(5)
N(1)–Fe–N(3)	88.89(5)
N(1)–Fe–N(5)	87.80(5)
N(3)–Fe–N(5)	86.96(5)
N(1)–Fe–N(3)#1	91.11(5)
N(1)–Fe–N(5)#1	92.20(5)
N(3)–Fe–N(5)#1	93.04(5)

as expected for a Fe(II) complex of a tpm ligand in the LS state. The pyrazole tilt angles (τ) range from −0.05° to 2.93° at 100 K, and the average intraligand and interligand N–Fe–N bond angles are 87.88° and 92.12°, respectively (Supporting Information, Table S2). Again, these values are all in the expected range for a LS complex of this type.

To investigate whether **2b** would display spin-state crossover behavior, an X-ray structure was also determined of the same crystal warmed to room temperature. In this case no significant changes in cell parameters, bond distances, or structure were noted that would suggest the onset of any spin-state crossover behavior.

Mössbauer Effect Study. As a further test of the gradual nature of the spin-state crossover and a transition temperature very near room temperature, the ^{57}Fe Mössbauer spectrum of **2** was measured at low temperature and again at room temperature. The spectra are shown in Figure 7 and the calculated parameters are presented in Table 7.

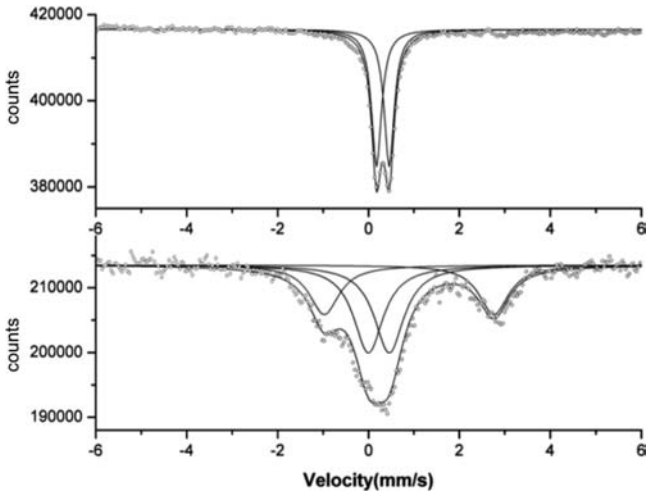

Figure 7. Mössbauer spectra of **2** at 77 K (top trace) and at 293 K (bottom trace).

Table 7. ^{57}Fe Mössbauer Parameters for Complex 2[a]

T (K)	Γ (mm/s)	QS (mm/s) (LS)	IS (mm/s) (LS)	QS (mm/s) (HS)	IS (mm/s) (HS)
298	0.79	0.48	0.22	3.78	0.85
77	0.26	0.28	0.28		

[a] Γ is the width at half-height, IS is the isomeric shift, and QS is the quadrupole splitting. The data were fit with two separate QSs at 298 K, indicated by numbers (1) and (2), while at 77 K a single set of parameters was necessary. Uncertainties in the fit are approximately 0.04 mm/s.

The spectra in Figure 7 show a transition from two lines at 77 K to four lines at 298 K with substantial line broadening. The low-temperature spectrum is a simple quadrupole doublet with a relatively small splitting, thus confirming the presence of only a LS complex. The high symmetry of the complex results in all 6 pyrazole moieties being equivalent, which allows application of a relatively simple model for determination of the sign of the quadrupole splitting (see Supporting Information).[19] At room temperature, the broadened spectrum is best interpreted as a mixture of two doublets. One of these doublets has parameters similar to those of the low temperature spectrum, while the other one has a much larger quadrupole splitting. This spectrum is a combination of LS and HS forms of the complex undergoing interconversion on a time scale similar to that of the Mössbauer measurement (ca. 10^{-7} s). Similar spectra have been observed by other researchers for similar complexes.[4a,d]

Solution Studies of 2. The UV–visible spectrum of **2** in acetonitrile was measured at a variety of temperatures and is shown in Figure 8. First, the solution is visibly purple, which indicates the presence of significant LS complex in solution. This color is the result of a weak ($\varepsilon \cong 110$ cm^{-1} M^{-1})

dx.doi.org/10.1021/ic2022038 | Inorg. Chem. 2012, 51, 1084–1093

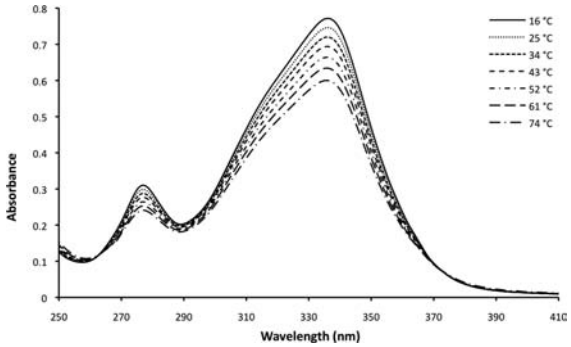

Figure 8. UV−vis spectra of **2** in CH_3CN showing the onset of spin-state crossover behavior.

absorbance band present near 18.8×10^3 cm^{-1} (530 nm) due to the $^1A_1 \rightarrow {}^1T_1$ transition in the LS complex. However, the much stronger MLCT band ($\varepsilon = 1.4 \times 10^4$ cm^{-1} M^{-1}) at 29.8×10^3 cm^{-1} (335 nm) is more useful for monitoring the spin-state of the complex by UV−visible spectroscopy. As can be seen in Figure 8, the intensity of this band decreases slowly with increasing temperature. Repeating the experiment in the presence of excess ligand **1** resulted in no change in the intensity of these bands, which is a clear indication that the absorbance decreases are due to spin changes (toward HS) and not to ligand dissociation. The bleaching of the band is moderate even at 69 °C, which shows that the conversion to HS has only just begun at these temperatures. These experiments show that while there is an unambiguous onset of spin-state crossover in solution, the temperature would have to be increased well beyond the boiling point of CH_3CN to achieve significant conversion to the HS state.

The ^1H NMR spectra of **2** in CD_3CN were recorded at both 23 and 60 °C, and the results are shown in Figure 9. The

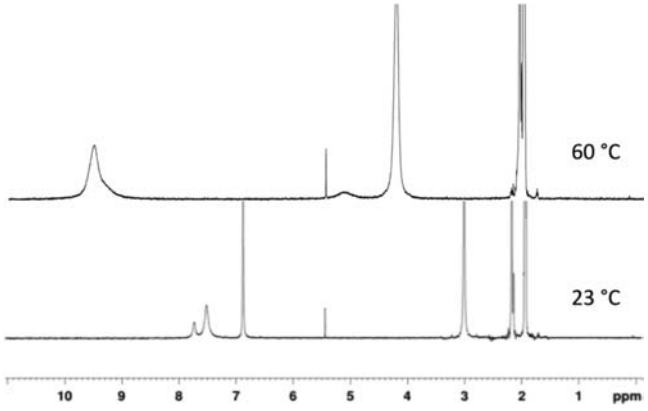

Figure 9. ^1H NMR spectrum of $Fe(\mathbf{1})_2^{2+}$ in CD_3CN at 23 °C (bottom) and 60 °C (top). The sharp peak near 5.5 ppm is methylene chloride.

spectrum at 23 °C reveals slightly broadened peaks with chemical shifts near those found for the free ligand; that is, there are no large paramagnetic shifts. Thus, the complex is largely LS at room temperature, but the slight broadening suggests that there has been an onset of spin-state crossover behavior in solution. In contrast, the spectrum at 60 °C shows broadened peaks with quite noticeable changes in chemical shifts. For example, the methine peak has shifted from 7.72 ppm and is now observed at 5.15 ppm. In fully HS tpm complexes of Fe(II), the methine proton has been observed as far upfield as −82.7 ppm.[3g,4f] The nearly diamagnetic spectrum at room temperature and the upfield shift of only ∼3 ppm as the temperature is increased to 60 °C supports the conclusions from the UV−visible experiments—the spin transition temperature ($T_{1/2}$) in solution is beyond the boiling point of acetonitrile and possibly in excess of 400 K.[3g]

DISCUSSION

The preparation of ligand **1** provides the first opportunity to cleanly isolate the influence of substituents placed in the 5-position from those in the 3-position on the spin-state crossover behavior in Fe(II)-tpm and -tp complexes. However, any comparison of spin-state crossover behavior based on solid-state data is necessarily complicated by the counterion and consideration of complex lattice effects. Perhaps this is best illustrated by the well-studied Fe(II) complex of tris(3,5-dimethylpyrazolyl)methane with a BF_4^- counterion, which undergoes a sharp spin transition at 206 K.[20] This behavior is the result of a phase change that leads to a cooperative spin-state transition of only half of the Fe(II) sites in the crystal. With iodide as a counterion, this same complex undergoes gradual spin-state crossover upon cooling starting at 195 K that ends by 70 K.[21]

In the present study, the BF_4^- and ClO_4^- salts (**2** and **2a**) have very similar crystal structures and transition temperatures ($T_{1/2} \sim 300$ K) in the solid state. There is also some indication of a modest cooperativity in the spin-state crossover in **2**, which is also likely to be present in **2a**. The cooperativity results in the spin-state transition occurring over a narrower temperature range than would otherwise be expected. The cooperativity is most likely the result of the deformations in the smaller LS crystal lattice that must occur to accommodate the developing HS complexes, which are larger. Once the lattice has started to expand, subsequent LS→HS transitions become less energetically costly and proceed more easily.

An important comparison to the present work is provided by the regioisomeric ligand bis(3-methylpyrazolyl)(5-methylpyrazolyl)methane.[4a] The Fe(II) complex of this ligand with a BF_4^- counterion also displays gradual spin-state crossover behavior. In this case, the solid-state behavior is somewhat similar to **2** and **2a**, but the $T_{1/2}$ is lowered to near 250 K. The simple explanation for the lower $T_{1/2}$ is the presence of substituents in two of the three 3-positions of each tpm ligand in this complex. All solid-state data collected to date suggest that substitution in the 3-positions of tpm and tp ligands substantially lowers the $T_{1/2}$ of the corresponding Fe(II) complexes because of steric repulsion of the interdigitated substituents, which presumably destabilizes the shorter Fe−N bonds of the LS complexes and favors the longer Fe−N bonds of the HS complexes. It is also apparent that any substituents in the 3-position that are much larger than a methyl destroy any hope of observing spin-state crossover behavior and essentially lock the complex into the HS form. Since ligand **1** has only H atoms in the 3-positions, on this basis alone spin-state crossover behavior with a relatively high $T_{1/2}$ might be expected in the Fe(II) complex.

Crystals of the BPh_3CN^- salt (**2b**) show no tendency to undergo spin-state crossover at room temperature, and in this sense its behavior is somewhat similar to the solution behavior of **2**. The $T_{1/2}$ differences between **2b** and **2a** (and **2**) show conclusively that when only considering solid-state data it is difficult to discern with any certainty the effect of substitution

dx.doi.org/10.1021/ic2022038 | Inorg. Chem. 2012, 51, 1084−1093

at the 5-position of the tpm ligand on the spin-state crossover behavior of the Fe(II) complex—counterion and lattice effects can be overwhelming. The solution behavior is a better indicator of the inherent tendency of a Fe-tpm or -tp molecular species to undergo spin-state crossover, as solvent effects are probably relatively minor when compared to crystal packing effects. In the case of **2**, the NMR results together with the UV−visible data show that there is an appreciable difference between the transition temperature in acetonitrile solution ($T_{1/2} \sim 400$ K) and that in the solid state for **2** and **2a**. In fact, the $T_{1/2}$ in solution for **2** is apparently higher than that of the unsubstituted Fe-tpm complex as measured by Reger et al.[4f] in DMF ($T_{1/2} = 345$ K) and Toftlund et al.[22] in acetonitrile ($T_{1/2} = 340$ K). Likewise, the unsubstituted Fe-tp complex shows a $T_{1/2}$ near 370 K.[23] On the other hand, the 3,5-dimethyl tpm complex is HS in solution and shows no evidence of spin-state crossover behavior at a temperature as low as 185 K—substitutents in the 3-position lower the $T_{1/2}$ of the Fe(II) complex. The results from **2** suggest that substitution at the 5-position may have the opposite effect—these seem to raise the HS−LS transition temperature above that of even the unsubstituted complex. One possible explanation for this result is that the methyls in the 5-position are aligned approximately parallel to each other and to the methine hydrogen. Repulsion of these groups would tend to close the bite of the ligand, thereby stabilizing the shorter Fe−N bond distances of the LS complex.

CONCLUSION

The synthesis of the new tpm ligand, tris(5-methylpyrazolyl)-methane (**1**), is reported. The synthesis can be accomplished in good yield by first tetra-lithiating unsubstituted tpm followed by trimethylation with methyl iodide. Various salts of the Fe(II) complex of the new ligand, $[Fe(\mathbf{1})_2]^{2+}$, were also synthesized and studied by X-ray diffraction, Mössbauer, UV−visible spectroscopy, and ^{1}H NMR. The BF_4^- and ClO_4^- salts display spin-state crossover in the solid state with a transition temperature near 300 K, while the BPh_3CN^- salt is LS even at room temperature. Onset of a spin transition is also observed in acetonitrile solution, but the transition temperature is probably closer to 400 K in this case. The data suggests that groups in the 5-position of a tpm ligand have a smaller but opposite effect on the HS−LS transition temperature of the Fe(II) complexes as compared to the same group placed at the 3-position of the ligand.

ASSOCIATED CONTENT

Supporting Information

Crystallographic data in CIF format. Further details are given in Figures S1−S4 and Tables S1−S2. This material is available free of charge via the Internet at http://pubs.acs.org.

AUTHOR INFORMATION

Corresponding Author

*E-mail: goodmams@buffalostate.edu.

ACKNOWLEDGMENTS

Financial support for this project was provided by Faculty Research Council, D'Youville College. D.J.M. and G.L. gratefully acknowledge the U.S. DOE Grant DEFG02-03ER46064 for support of their work.

REFERENCES

(1) (a) Santini, C.; Pellei, M.; Lobbia, G. G.; Papini, G. *Mini-Rev. Org. Chem.* **2010**, *7*, 84. (b) Bigmore, H. R.; Lawrence, S. C.; Mountford, P.; Tredget, C. S. *Dalton Trans.* **2005**, *4*, 635. (c) Trofimenko, S. *Scorpionates: The Coordination Chemistry of Polypyrazolylborate Ligands*; Imperial College Press: River Edge, NJ, 1999. (d) Reger, D. L. *Comments Inorg. Chem.* **1999**, *21*, 1. (e) Trofimenko, S. *Chem. Rev.* **1993**, *93*, 943. (f) Trofimenko, S. *Prog. Inorg. Chem.* **1986**, *34*, 141. (g) Trofimenko, S. *J. Am. Chem. Soc.* **1967**, *89*, 3148. (h) Trofimenko, S. *J. Am. Chem. Soc.* **1970**, *92*, 5118.

(2) (a) Cushion, M. G.; Meyer, J.; Heath, A.; Schwarz, A. D.; Fern, I.; Breher, F.; Mountford, P. *Organometallics* **2010**, *29*, 1174. (b) Fernandez, I.; Burgos, P. O.; Armbruster, F.; Krummenacher, I.; Breher, F. *Chem. Commun.* **2009**, *18*, 2586. (c) Kuzu, I.; Krummenacher, I.; Hewitt, I. J.; Lan, Y.; Mereacre, V.; Powell, A. K.; Hoefer, P.; Harmer, J.; Breher, F. *Chem.—Eur. J.* **2009**, *15*, 4350. (d) Byers, P. K.; Carr, N.; Stone, F.; Gordon, A. *J. Chem. Soc., Dalton Trans.* **1990**, *12*, 3701.

(3) (a) Shakirova, O. G.; Lavrenova, L. G.; Kurat'eva, N. V.; Naumov, D. Y.; Daletskii, V. A.; Sheludyakova, L. A.; Logvinenko, V. A.; Vasilesvskii, S. F. *Russ. J. Coord. Chem.* **2010**, *36*, 275. (b) Dhanalakshmi, T.; Suresh, E.; Palaniandavar, M. *Dalton Trans.* **2009**, *39*, 8317. (c) Salaudeen, A. A.; Kilner, C. A.; Halcrow, M. A. *Polyhedron* **2008**, *27*, 2569. (d) Edwards, P. G.; Harrison, A.; Newman, Pau.D.; Zhang, W. *Inorg. Chim. Acta* **2006**, *359*, 3549. (e) Long, G. J.; Grandjean, F.; Reger, D. L. *Top. Curr. Chem.* **2004**, *233*, 91. (f) Field, L. D.; Messerle, B. A.; Soler, L. P.; Hambley, T. W.; Turner, P. *J. Organomet. Chem.* **2002**, *655*, 146. (g) Reger, D. L.; Little, C. A.; Rheingold, A. L.; Sommer, R.; Long, G. J. *Inorg. Chim. Acta* **2001**, *316*, 65.

(4) (a) Reger, D. L.; Elgin, J. D.; Foley, E. A.; Smith, M. D.; Grandjean, F.; Long, G. J. *Inorg. Chem.* **2009**, *48*, 9393. (b) Moubaraki, B.; Leita, B. A.; Halder, G. J.; Batten, S. R.; Jensen, P.; Smith, J. P.; Cashion, J. D.; Kepert, C. J.; Letard, J. F.; Murray, K. S. *Dalton Trans.* **2007**, *39*, 4413. (c) Reger, D. L.; Gardinier, J. R.; Elgin, J. D.; Smith, M. D. *Inorg. Chem.* **2006**, *45*, 8862. (d) Reger, D. L.; Elgin, J. D.; Smith, M. D.; Grandjean, F.; Rebbouh, L.; Long, G. J. *Eur. J. Inorg. Chem.* **2004**, *16*, 334. (e) Batten, S. R.; Bjernemose, J.; Jensen, P.; Leita, B. A.; Murray, K. S.; Moubaraki, B.; Smith, J. P.; Toftlund, H. *Dalton Trans.* **2004**, *20*, 3370. (f) Reger, D. L.; Little, C. A.; Rheingold, A. L.; Lam, M.; Liable-Sands, L. M.; Rhagitan, B.; Concolino, T.; Mohan, A.; Long, G. J.; Briois, V. *Inorg. Chem.* **2001**, *40*, 1508. (g) Anderson, P. A.; Astley, T.; Hitchman, M. A.; Keene, F. R.; Moubaraki, B.; Murray, K. S.; Skelton, B. W.; Tiekink, E. R. T.; Toftlund, H.; White, A. H. *Dalton Trans.* **2000**, *20*, 3505.

(5) (a) Joachim, C.; Gimzewski, J. K.; Aviram, A. *Nature* **2000**, *408*, 541. (b) Kahn, O.; Martinez, C. J. *Science* **1998**, *279*, 44. (c) Létard, J.-F.; Guionneau, P.; Goux-Capes, L. *Top. Curr. Chem.* **2004**, *235*, 221.

(6) (a) Reger, D. L.; Grattan, T. C.; Brown, K. J.; Little, C. A.; Lamba, J. J. S.; Rheingold, A. L.; Sommer, R. D. *J. Organomet. Chem.* **2000**, *607*, 120. (b) Reger, D. L.; Collins, J. E.; Jameson, D. L.; Castellano, R. K.; Canty, A. J.; Jin, H. *Inorg. Synth.* **1998**, *32*, 63. (c) Pettinari, C.; Pellei, M.; Cingollani, A.; Martini, D.; Drozdov, A.; Troyanov, S.; Panzeri, W.; Mele, A. *Inorg. Chem.* **1999**, *38*, 5777.

(7) Sheldrick, G. M. *SADABS*, version 2007/4; University of Göttingen: Göttingen, Germany, 2007.

(8) Altomare, A.; Burla, M. C.; Camalli, M.; Cascarano, G. L.; Giacovazzo, C.; Guagliardi, A.; Moliterni, A. G. G.; Polidori, G.; Spagna, R. *SIR97: A new program for solving and refining crystal structures*; Istituto di Cristallografia, CNR: Bari, Italy, 1999.

(9) Sheldrick, G. M. *Acta Crystallogr.* **2008**, *A64*, 112−122.

(10) DeMarco, M.; Cao, G.; Crow, J.; Coffey, D.; Toorongian, S.; Haka, M.; Fridmann, J. *Phys. Rev. B* **2000**, *62*, 14297.

(11) (a) Silva, T. F. S.; Mishra, G. S.; Guedes da Silva, M. F. C.; Pombeiro, A. J. L. *Dalton Trans.* **2009**, *42*, 9207. (b) McLachlan, C. C.; Weberski, M. P.; Greiner, B. A. *Inorg. Chim. Acta* **2009**, *362*, 2662. (c) Liddle, B. J.; Gardinier, J. R. *J. Org. Chem.* **2007**, *72*, 9794. (d) Reger, D. L.; Foley, E. A.; Semeniuc, R. F.; Smith, M. D. *Inorg. Chem.* **2007**, *46*, 11345.

(12) Reger, D. L.; Grattan, T. C. *Synthesis* **2003**, *3*, 350.
(13) Diez-Barra, E.; de la Hoz, A.; Sanchez-Migallon, A.; Tejada, J. *J. Chem. Soc., Perkin Trans. 1* **1993**, *9*, 1079.
(14) (a) Gutlich, P.; Hauser, A.; Spiering, H. *Angew. Chem., Int. Ed. Engl.* **1994**, *33*, 2024. (b) Gutlich, P. In *Mossbauer Spectroscopy Applied to Inorganic Chemistry*; Long, G. J., Ed.; Plenum: New York, 1984; Vol. *1*, p 287.
(15) (a) Schneider, C. J.; Moubaraki, B.; Cashion, J. D.; Turner, D. R.; Leita, B. A.; Batten, S. R.; Murray, K. S. *Dalton Trans.* **2011**, *40*, 6939. (b) Guionneau, P.; Marchivie, M.; Bravic, G.; Létard, J.-F.; Chasseau, D. *Top. Curr. Chem.* **2004**, *234*, 97.
(16) (a) Reger, D. L.; Little, C. A.; Semeniuc, R. F.; Smith, M. D. *Inorg. Chim. Acta* **2009**, *363*, 303. (b) Reger, D. L.; Elgin, J. D.; Smith, M. D.; Grandjean, F.; Rebbouh, L.; Long, G. J. *Polyhedron* **2006**, *25*, 2616. (c) Reger, D. L.; Gardinier, J. R.; Smith, M. D.; Shahin, A. M.; Long, G. J.; Grandjean, F. *Inorg. Chem.* **2005**, *44*, 1852. (d) Reger, D. L.; Gardinier, J. R.; Gemmill, W.; Smith, M. D.; Shahin, A. M.; Long, G. J.; Rebbouh, L.; Grandjean, F. *J. Am. Chem. Soc.* **2005**, *127*, 2303. (e) Reger, D. L.; Little, C. A.; Smith, M. D.; Long, G. J. *Inorg. Chem.* **2002**, *40*, 2870.
(17) Gütlich, P.; Garcia, Y.; Goodwin, H. A. *Chem. Soc. Rev.* **2000**, *29*, 419.
(18) Slichter, C. P.; Drickamer, H. G. *J. Chem. Phys.* **1972**, *56*, 2142.
(19) (a) Bancroft, G. M. *Coord. Chem. Rev.* **1973**, *11*, 247. (b) Bancroft, G. M. *Mössbauer Spectroscopy – An Introduction for Inorganic Chemists and Geochemists*; McGraw-Hill: London, U.K., 1973.
(20) Reger, D. L.; Little, C. A.; Smith, M. D.; Long, G. J. *Inorg. Chem.* **2002**, *41*, 4453.
(21) Reger, D. L.; Little, C. A.; Smith, M. D.; Rheingold, A. L.; Lam, K.-C.; Concolino, T. L.; Long, G. J.; Hermann, R. P.; Grandjean, F. *Eur. J. Inorg. Chem.* **2002**, 1190.
(22) McGarvey, J. J.; Toftlund, H.; Al-Obaidi, A. H. R.; Taylor, K. P.; Bell, S. E. J. *Inorg. Chem.* **1993**, *32*, 2469.
(23) Beattie, J. K.; Binstead, R. A; West, R. J. *J. Am. Chem. Soc.* **1978**, *100*, 3044.